Journal of Marine Science and Technology (2020) 25:1151–1165
https://doi.org/10.1007/s00773-020-00706-9

ORIGINAL ARTICLE

A numerical investigation on the effect of symmetric and asymmetric flooding on the damage stability of a ship

XinLong Zhang[1] · Zhuang Lin[1] · Ping Li[1] · DengKe Liu[1] · Ze Li[1] · ZhanWei Pang[1] · MeiQi Wang[1]

Received: 23 July 2019 / Accepted: 4 February 2020 / Published online: 17 February 2020

Abstract
Reliable analysis of the flooding process and motion responses onboard a damaged ship is extremely significant for assessing the remaining survivability and improving the damage stability. This study implemented the Unsteady Reynold-Average Navier–Stokes (URANS) solver to monitor the three degrees of freedom (DOF) motion, investigating the effect of symmetric and asymmetric flooding on the damage stability. The Volume of Fluid (VOF) method was applied to visualize the flooding process and capture the complex hydrodynamics behavior. Additionally, basic governing equations of fluid flow and free motion are detailed. The simulation results show that in the same damage condition, the transverse asymmetric flooding results in a larger heel angle. However, for the pitch and heave motion, there are small differences between the symmetric flooding and asymmetric flooding. Therefore, if the damaged ship is predicted to keep afloat, the transverse symmetric flooding should be guaranteed as much possible. In this case, the flooding water can flow from the damaged side to the intact side. Consequently, the damaged ship can maintain a relatively stable floating state, decreasing the risk of capsizing due to the excessive heel angle. Finally, all the numerical simulation cases are performed on the commercial software CD Adapco STAR-CCM+.

Keywords Symmetric/asymmetric flooding · VOF · URANS · Flooding process · Damage stability

1 Introduction

Flooding in ships is usually a result of damage caused by collision, grounding or violent interaction with the unpredictable sea environment (wind, current and waves). When a ship is damaged for any of the aforementioned reasons, its structural integrity and water tightness are partially lost. In a real damage scenario, different compartment layouts result in distinct flooding forms, and the motion responses of the damaged ship are characterized. Thus, a clear understanding of the motion responses under various flooding forms is crucial to properly assess the remaining survivability for a damaged ship. Recently, many efforts have also been made to study the survivability and safety assessment of damaged ships, including developing the numerical simulation method to capture the flooding process and predict the motion responses, as well as performing the model tests to validate the numerical reliability [1]. At the same time, the hydrodynamic problems in the flooding process have been a major issue as summarized in the last several International Towing Tank Conferences (ITTC) [2, 3].

In order to investigate the flooding process and the motion responses of a damaged cruiser, Cho et al. [4] performed a series of experimental tests and numerical simulations in calm water and waves. The established model considers the dynamics of free surface as the ship motion. Korkut et al. [5] explored the effect of the damage and varying wave heights on the motion responses of the experimental models. The obtained results indicate that the damage has an adverse effect on the motion responses of the model depending upon the directionality of the waves and frequency range applied. Acanfora et al. [6] conducted an experimental campaign on a passenger ferry hull with a realistic arrangement of the flooded compartment. The effects of obstacles in the engine room compartment, such as decks and engines, on ship roll responses, are studied. Domeh et al. [7] studied how variations of compartment permeability and internal configuration, together with orifice size, affect the damaged ship motion response to waves. Siddiqui et al. [8] performed

✉ Zhuang Lin
linzhuang@hrbeu.edu.cn

[1] College of Shipbuilding Engineering, Harbin Engineering University, Harbin 150001, China

a detailed series of experiments in a wave flume on a thin walled prismatic hull form. Forced oscillatory heave tests in calm water have been carried out by varying the model-motion parameters and examining both intact and damaged conditions. The obtained results demonstrate occurrence of sloshing and piston mode resonances in the tests and their influence on the hydrodynamics loads of a damaged ship. Lee et al. [9] performed well-designed model tests for building a database for Computational Fluid Dynamics (CFD) validation. Through the free roll decay tests, the effects of the flooding water on the roll decay motion of a damaged ship were investigated. Manderbacka et al. [10] performed model tests to generate validation data for the numerical codes predicting the sloshing and progression of water through an opening. Models tests concentrated purely on the internal sloshing motion under forced compartment motions, thus uncoupling the ship's motion response. Generally, these model experiments can accurately monitor the motion responses and assess the damage stability in the specified damaged scenario. However, model tests cannot tackle multiple damage cases efficiently and economically.

During the past two decades, owing to the improvements in high-performance computers, application of CFD methods may be a viable alternative approach. A numerical tool combined with the Navier–Stokes (NS) solver was developed to simulate water flooding into a damaged ship. The VOF method is applied to capture the air–fluid interface [11]. Haro et al. [12] investigated the motion responses and flooding behavior of a damaged passenger ship model by solving URANS equations, using CFD Ship-Iowa program and SUGGAR + + library. The CFD analysis was designed with consideration to the Safe Return to Port (SRTP) regulation, and the effect of wave conditions and flooded water behaviors on the motion and propulsion characteristics of the ship were investigated. Sadat-Hosseini et al. [13] conducted URANS simulations for zero-speed damaged passenger ship in calm water and waves with 6DOF motions including flooding procedure in calm water, roll decay in calm water and motions in regular beam waves for various wavelengths. Ming et al. [14] carried out a numerical study regarding the damaged ship cabin flooding in transversal regular waves. This numerical simulation is based on a weakly compressible Smooth Particle Hydrodynamics (WCSPH) method. Zhang et al. [15] focused on the application of Reynolds-Averaged Navier–Stokes (RANS) solver combined with the VOF method for analyzing the effect of air compression on the flooding process and motion responses. The flooding processes in different damaged scenarios are well visualized. The obtained flooding time can provide necessary data support for appropriate rescue management and evacuation options [16]. Celis et al. [17] used the volume fraction equation to capture air–water interface displacement in order to investigate the hydrodynamics phenomena in the flooding process. The implemented numerical scheme is based on the finite difference, where the Euler equations are solved using an upwind total variation diminishing scheme with a structured computational mesh. In addition, some numerical codes are developed to assess the damage stability. Santos et al. [18] described a mathematical model in the time domain of the motions and flooding of ships in a seaway. The effect of parametric variations of different factors on the ship's survivability are assessed. The equations of ship motion are solved using a fourth-order Runge–Kutta method. The amount of the flooded water and the forces caused by the floodwater located inside the ship's compartment are calculated using the hydraulic model based on the Bernoulli equation. A numerical non-linear time domain simulation based on the lumped mass method was applied to investigate the flooding process and transient response of a ship to abrupt flooding. The ship and floodwater motions are fully coupled while the variation of the flooded water mass and the transporting the momentum by the flooding ingress are accounted for [19]. Manderbacka et al. [20] studied roll decay of a ship in flooded condition numerically. Floodwater motions in the compartments were simulated by applying lumped mass with a moving free surface method. Water exchange through the non-watertight bulkheads in compartment was modeled by applying the hydraulic equation. Acanfora et al. [21] developed and presented a fast simulation method based on the lumped mass approach. The method applies to both the transient stage of flooding and to the dynamic behavior of a flooded ship in regular waves. Fonfach et al. [22] considers two methods to analyse the strongly nonlinear sloshing flow coupled to the flooding problems. The first method is the lumped mass method. The second one is a Lagrangian based code, specifically the moving particle semi-implicit (MPS) method. The application of two numerical methods focuses on the calculation of the volume transfer between two contiguous compartments and its effects on the hydrodynamic forces at several sloshing and flooding conditions. Generally, these numerical simulation methods have been proven to provide convenience and reliability for damage flooding researches.

In this paper, the numerical simulation based on URANS solver is applied to investigate the influence of the flooding forms on the motion responses. The surface processing technique (volume of fluid method) has been applied to visualize the free surface during flooding. The paper is organized as follows: in Sect. 2, the basic governing equations applied in solver are discussed; in Sect. 3, the potential damage location of the ship is elaborated; in Sect. 4, the hydrodynamic characteristics in the flooding process are analyzed; in Sect. 5, the established DTMB 5415 model is described; in Sect. 6, the relevant numerical conditions are detailed, including the mesh type, physical models and solver settings; in Sect. 7, the 3-DOF motion responses of

the damaged ship under different flooding forms are investigated, including roll, pitch and heave motion; in Sect. 8, some important conclusions are enclosed.

2 Methodology

2.1 Governing equations of fluid flow

During modeling physics, the Multiphase model is used to solve the flow and the interaction of water and air phases within the same system where distinct interfaces exist between the phases. This applied model solves conservation equations for mass, momentum for each phase. Phase (*i* and *j*) interaction models are provided to define the influence that one phase exerts upon another across the interfacial area between them [23]. The specified conservation equations of mass and momentum are, respectively, presented as Eqs. 1 and 2.

$$\frac{\partial}{\partial t}\left(\alpha_i\rho_i\right)+\nabla\cdot\left(\alpha_i\cdot\rho_i\cdot v_i\right)=\sum_{i\neq j}\left(m_{ij}-m_{ji}\right)+S_i^{\alpha} \tag{1}$$

$$\frac{\partial}{\partial t}\left(\alpha_i\rho_i v_i\right)+\nabla\cdot\left(\alpha_i\rho_i v_i v_i\right)=-\alpha_i\nabla p+\alpha_i\rho_i g+\nabla\cdot\left[\alpha_i\left(\tau_i+\tau_i^t\right)\right]+M_i+\left(F_{\text{int}}\right)_i+S_i^v+\sum\left(m_{ij}v_j-m_{ji}v_i\right) \tag{2}$$

where, α_i is the volume fraction of phase i; ρ_i is the density of phase i; v_i is the velocity of phase i; S_i^{α} is the phase mass source term; m_{ij} is the mass transfer rate to phase i to phase j; m_{ji} is the mass transfer rate to phase i from phase j; p is the pressure; g is the gravity vector;τ_i and τ_i^t are the interphase momentum transfer stresses, respectively; M_i is the interphase momentum transfer per unit volume; S_i^v is the phase momentum source term; $\left(F_{int}\right)_i$ represents the internal forces.

2.2 Governing equations of free motion

In the applied numerical approach, the damaged ship is considered as a rigid body in which the relative distance between internal points does not change. By using a Cartesian coordinate system, the rigid body is able to translate along all three axes (surge, heave and sway) and rotate about them (roll, pitch and yaw), giving the six degrees of freedom. As shown in Fig. 1, in order to describe the translation and rotation motion of the rigid body, three necessary coordinate systems are defined respectively. The Laboratory Coordinate System is automatically generated when the geometric surface of the damaged ship is imported into the software. Its origin position is same as the origin position set in the modeling process. Due to its stationary nature and the origin not being the center of mass, it cannot be applied to monitor the motions of the rigid body. It is mainly used to define the specified point like the center of mass, the simulation domain and some refinement blocks. The other two coordinate systems are created at the center of the body mass. The Body Local Coordinate System is also automatically generated when the properties of the damaged ship are specified in the 6-DOF solver. It can move as the rigid body's motion. However, the stationary Initial Orientation Coordinate System needs to be created manually and assigned to define the correct orientation of the 6-DOF body in its initial position. In this case, when the rigid body moves under the excitation of the external forces, the origin position differences between Initial Orientation Coordinate System and Body Local Coordinate System can be converted to present the translation distance of the rigid body. The modified Euler angles between the current direction of the axis and the original direction of the axis can be applied to monitor the rotation of the rigid body. For moving axes in this paper, the order of rotations (*XYZ* Axis) needs to read from back to front. The first rotation is about the z axis. The second is around the y axis of the new coordinate system created by rotating the system around the z axis. The third rotation is about the x axis of another new coordinate system created by rotating the previous system around its y axis. The rigid body's position is updated by the continuous numerical integration. For the damaged ship, motion can be modelled using a center of mass and moments of inertia of the ship around the fixed center of mass. The resultant forces and moments acting on the damaged ship are used to calculate the motion along axes as well as angular rotation motion and orientation of the body. The specified equations are presented as Eqs. 3 and 4.

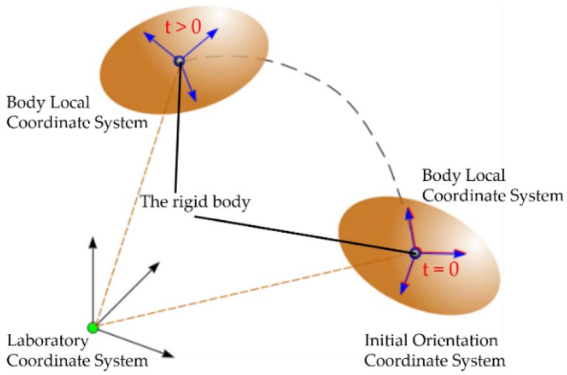

Fig. 1 Three necessary coordinate systems for the rigid body motion

$$m\frac{\mathrm{d}\boldsymbol{v}}{\mathrm{d}t}=\boldsymbol{f}, \tag{3}$$

$$\boldsymbol{M}\frac{\mathrm{d}\omega}{\mathrm{d}t} + \omega \times \boldsymbol{M}\omega = \boldsymbol{n}, \tag{4}$$

$$M = \begin{bmatrix} M_{xx} & M_{xy} & M_{xz} \\ M_{xy} & M_{yy} & M_{yz} \\ M_{xz} & M_{yz} & M_{zz} \end{bmatrix} \tag{5}$$

where, m represents the mass of the ship; $\boldsymbol{v}$ is the velocity of centre of mass; ω is angular velocity of the ship. $\boldsymbol{M}$ is a symmetric tensor of the moments of inertia illustrated in Eq. 5. It can be defined using six variables: specifying diagonal moments $\left(M_{xx}, M_{yy}, M_{zz}\right)$ and specifying off diagonal moments $\left(M_{xy}, M_{yz}, M_{xz}\right)$. $\boldsymbol{f}$ and $\boldsymbol{n}$ are the resultant force and moment acting on the ship. Forces and moments acting on the ship due to fluid flow are calculated as a function of both pressure forces ($\boldsymbol{f}_p$ and $\boldsymbol{n}_p$) and shear forces ($\boldsymbol{f}_\tau$ and $\boldsymbol{n}_\tau$) acting on the ship boundaries. The external forces ($\boldsymbol{f}_{\mathrm{ext}}$) and moments ($\boldsymbol{n}_{\mathrm{ext}}$) can be defined and contribute in the summation of forces, e.g. gravity ($\boldsymbol{f}_g$) or propeller models. Therefore, the resultant forces and moments acting on the ship can be presented as Eqs. 6 and 7.

$$\mathbf{f} = f_r\left(\boldsymbol{f}_p + \boldsymbol{f}_\tau + \boldsymbol{f}_g + \sum \boldsymbol{f}_{\mathrm{ext}}\right) \tag{6}$$

$$\mathbf{n} = f_r\left(\boldsymbol{n}_p + \boldsymbol{n}_\tau + \sum \boldsymbol{n}_{\mathrm{ext}}\right) \tag{7}$$

where, f_r is the ramping factor that can be applied to external forces and moments on the body that are induced by the fluid flow on the ship and to the gravity force. It is recommended that in the case of rigid body motions, a period of settling into a steady flow regime is implemented before any excitations (e.g. waves) are added [24]. It can smooth transient motions due to inaccuracies inherent in initial conditions. With the values of release time t_s and ramp time t_r, the ramping factor function is defined as follows.

$$f_r = \begin{cases} 0 : t < t_s \\ \frac{t - t_s}{t_r} : t_s \le t < t_s + t_r \\ 1 : t \ge t_s + t_r \end{cases} \tag{8}$$

In an unsteady model, the release time allows some time to initialize the fluid flow. The typical range would be 10–50 time-steps. At release time, force and moments are applied to the body and can cause a shock effect. Applying a ramp time applies the forces and moments proportionally across the interval to reduce the shock effect. The value of the ramp time is typically 10 times the release time. For the simulations in this paper, the damaged ship is placed in the still water. Therefore, there is no need to consider the effect of the fluid flow initialization. The release time and the ramp time are set to be 0 while the ramping factor f_r is always going to be 1. In this case, when the damage flooding occurs, the resultant forces and moments acts on the damaged ship at the beginning of the simulation. As soon as the flooding water flooded into the damaged compartment, the damaged ship moves.

3 Potential damage location of the ship

After analyzing a large number of damage cases, the potential damage locations are presented in Fig. 2. Taking a cross section of the ship for an example, the entire cross sectional area is divided into four regions by two vertical limit lines and one horizontal limit line. Compartments close to hull sides may be damaged by collision or severe impact, and the main damage positions are on either side of the compartments. Once the side damage flooding occurs, the specific damage position can be determined based on the direction of the transient heel angle. Norwegian "KNM Helge Ingstad" frigate (2018) is an example where the frigate collided with the giant oil tank. The frigate sustained major damage in the collision, leading to flooding, water accumulation and finally capsizing with loss of stability. Actually, the collision specified in SOLOAS90 can reach the penetration limit of B/5. If the compartments are completely within the B/5 limit lines and above the double bottom, the potential damages are considered to be at the bottom of the compartments, and are due to the bottom grounding. Costa Concordia (2012) is another example of a ship disaster. The cruise ship capsized after it struck rocks off the Coast of Giglio Island in the Tyrrhenian Sea, leading 32 people to die. From a large amount of bottom grounding data, Bulian et al. [25] derives that 90% of the bottom grounding cases are limited to a vertical H below.

$$H = 0.55 \cdot \min\left(0.503B^{0.636}, T\right) \tag{9}$$

where, B is the width of the ship, and T is the design draught. Therefore, the compartments below the height (H) are more likely to be damaged by grounding. Compartments that exceed the height H, and are within the B/5 limit-lines will not be damaged by collision or grounding. The flooding

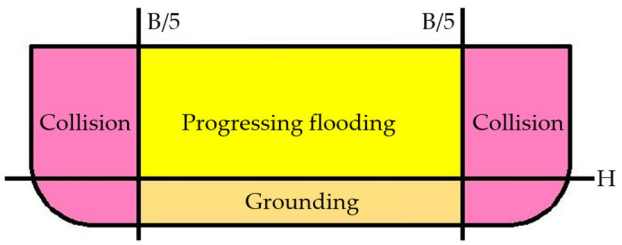

Fig. 2 Sketch of potential damage regions

water in these compartments may spread from other damaged compartments. Or the flooding water may be caused by further leakage or collapse of internal structures, when the hydrostatic pressure in the damaged compartment exceeds the structural tolerance limit.

It is worth noting that when the damage flooding occurs due to a collision, different internal layouts will result in different flooding forms, including symmetric flooding and asymmetric flooding. As shown in Fig. 3, if the internal layout allows the flooding water to flow from the damaged side to the intact side, the symmetric flooding is created. The damaged ship can maintain a stable floating state with a small heel angle. However, the increase of flooding water will worsen the sinkage of the damaged ship. If the flooding is blocked by the internal layout, the asymmetric flooding is created. The damaged ship remains with a large heel angle, which may increase the risk of capsizing. The following simulation cases in this paper will elaborate the specified effects of two flooding forms on the damaged stability, including roll, pitch and heave motion.

4 Analysis of the flooding characteristics

In the same damage condition, the symmetric flooding scenario usually has a larger flooding space than the asymmetric flooding scenario. The larger space allows for sufficient progression of the flooding water. Therefore, the symmetric flooding scenario can provide enough possibility for visualizing more hydrodynamic phenomena in the flooding process. In this section, the flooding characteristics are analyzed by a typical flooding process of the middle symmetric flooding scenario. In general, the flooding process can be divided into three separate stages with different characteristics, including transient stage, progressive flooding stage and steady state. The first stage is called the transient stage as shown in Fig. 4a, involving complex hydrodynamic phenomena. When the water ingress flows from the damaged side to the intact side, the flooding water will impact the hull plate, causing splash and tumble behavior. Also, the bubble phenomenon is formed between the flooding water and the compressed air without timely escaping from the flooded compartment. This stage is often more dangerous, and the damaged ship may be accompanied with obvious sloshing due to the additional momentum generated by the transient flooding water. However, the transient stage is relatively short and only lasts for several roll cycles or seconds. Then, the flooding water gradually enters the compartment under the effect of the hydrostatic pressure difference between the inside and outside of the damaged compartment. This process of continuously increasing the flooding water can be called the progressive flooding stage as shown in Fig. 4b. During the progressive flooding stage, the flooding water enters the damaged compartment at a relatively slow rate, and the fluctuation of the free surface is not as violent as the transient flooding stage. In addition, attention should be paid to investigate the influence of the flooding pressure on the internal structure. Jalonen et al. [26] studied the leakage and collapse of non-watertight doors under the flooding water pressure. The experimental results present the maximum flooding water levels that A-class structures and B-class structures can withstand. It is crucial for determining the flooding water how to evolve, as the bearing capacity of different local components are different. Finally, if the damaged ship does not capsize or sink, the ship will eventually maintain a steady state as shown in Fig. 4c. The height of the free surface in the damaged compartment is consistent with the external sea. The development of the entire flooding stages is based on the fact that the damage ship can survive the previous stage. Meanwhile, the established model has been simplified to a certain extent. The flooded compartments are assumed to be empty, not considering the effect of the compartment permeability on the flooding process. Some local structures that can modify the flow of the flooding water are not taken into account, such as stiffeners, web, brackets, etc.

5 Description of DTMB 5415 model

Several flooding cases have been carried out for the well-known benchmark US Navy Destroyer Hull DTMB 5415. The main particulars of the scale model (1/25) are given in Table 1 while the body plan and the view of the scale model are, respectively, in Figs. 5 and 6. In the modeling process, only the motion responses of the bare hull under the excitation of water ingress are taken into account, ignoring the effect of superstructures on the calculating results.

As shown in Fig. 7, four comparative damage scenarios were modeled separately. In order to eliminate the effects of air compression on the flooding process and the motion responses, the damaged compartment in each scenario is equipped with the ventilation hole. In Zhang [15], Ruponen

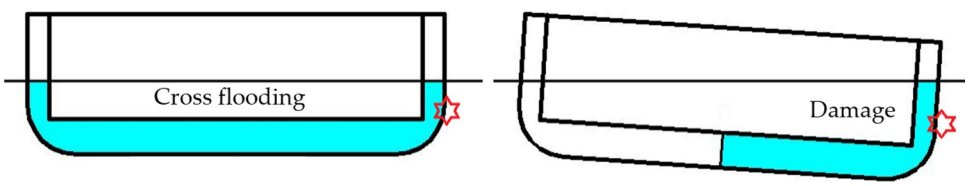

Fig. 3 Symmetric and asymmetric flooding for a bulk cargo ship

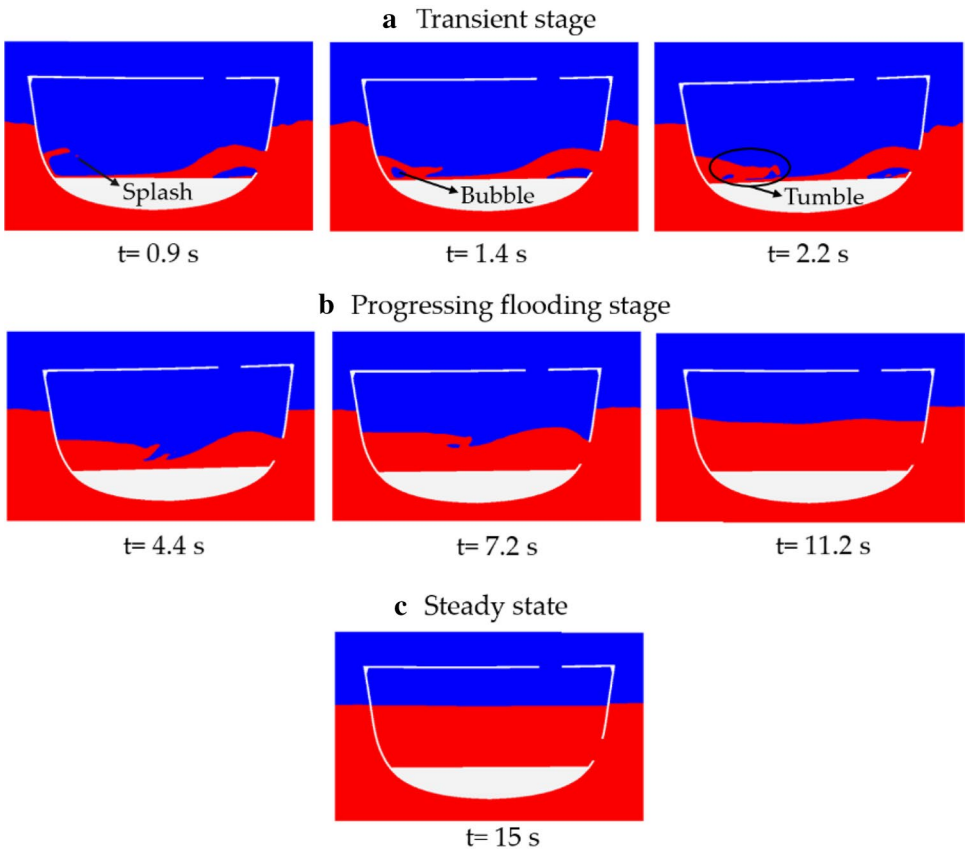

Fig. 4 Visualization of the middle symmetric flooding process

Table 1 Main particulars of US Navy Destroyer Hull 5415

Parameters	Particulars	Real ship	Scale model (1/25)
Length overall	L_{OA} (m)	151.1800	6.0472
Length between perpendiculars	L_{pp} (m)	142.0400	5.6856
Breadth at waterline	B_{WL} (m)	20.0300	0.8012
Depth to public spaces deck	D (m)	12.7400	0.5096
Design draft	T (m)	6.3100	0.2524
Volume	V (m^3)	8811.94	0.5640
Maximum section area	A_X (m^2)	96.7923	0.1549
Block coefficient	C_B	0.4909	0.4909
Prismatic coefficient	C_P	0.6409	0.6409
Midship section coefficient	C_M	0.7658	0.7658
Height of metacenter above keel	KM (m)	9.4700	0.3788
Height of centre of gravity above keel	KG (m)	6.2830	0.2513
Metacentric height	GM (m)	3.1870	0.1272

[27], Cao [28] and Palazzi [29], the effects of the air compression characteristics on the flooding time and damage stability have been systematically investigated. Hence, only damage scenarios with well ventilation are considered. In addition, four simulation cases can be defined from two aspects: damage location and internal layout. When the amidship damage occurs, the presence of a longitudinal bulkhead will determine whether the flooding water can flow from the damaged side to the other side. If the damaged compartment has no the longitudinal bulkhead, the flooding water can flow from the damaged side to the intact side, creating the symmetric flooding. The damaged compartment equipped with the longitudinal bulkhead makes the flooding water only accumulate on the damage side, creating the asymmetric flooding. The resulting distinction will form a contrast between symmetric and asymmetric flooding for the roll motion. For the pitch motion, due to the inherent property of the amidship damage, the pitch motion will not

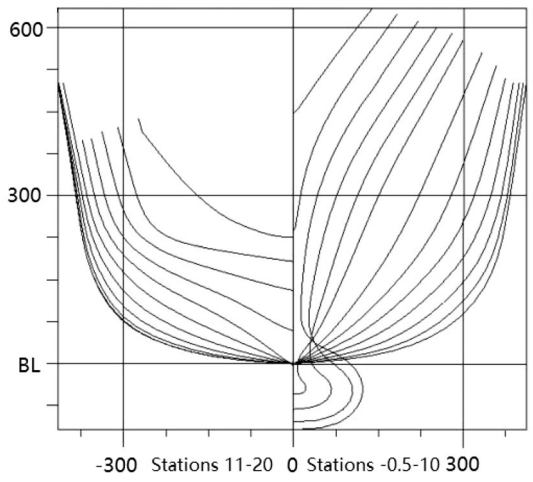

Fig. 5 Body plan of DTMB 5415 model (Unit: inch)

be able to clearly express the effect of flooding forms on the damage stability. The reason is that the amidship flooding is always symmetric to the pitch motion regardless of the transverse flooding forms. However, when the damage occurs near the bow, the pitch motion is always asymmetric. The transverse flooding form is determined by the presence of the longitudinal bulkhead. When the longitudinal bulkhead is provided, the transverse flooding is asymmetric. On the contrast, the flooding water will be symmetric while the increased flooding water will worsen the heave motion relative to the asymmetric flooding. These details will be elaborated from the following simulation results.

In order to simulate the motion of the damaged ship according to the forces induced by the flow, the Dynamic Fluid Body Interaction (DFBI) Rotation and Translation model is activated, and DFBI node is added to the simulation tree. Before performing the flooding simulations, the properties of the damaged hull need to be defined, including the weight, the center of mass and inertia moments. Table 2 listed the properties of the modeled hulls and the size of the openings in different scenarios. It can be found that different internal layouts will result in different hull weights, and the resulting initial drafts are characterized. In this paper, an accurate initial draft is firstly determined by assigning a specific weight to the intact 5415 model (Fig. 6). The initial height of the free surface is set to be 0.3 m. Only the heave motion is released, the final stable value is the actual draft. Such an operation is based on the principle that the displacement will be equal to the hull weight. Although the draft differences between the damage scenarios are small, the accurate initial drafts can ensure that when the simulation runs, the damaged hull will not heave up and down due to the difference between the displacement and hull height. The specific simulation results for the actual drafts are shown in

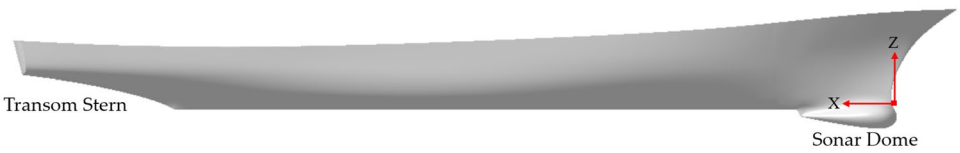

Fig. 6 A perspective view of the DTMB 5415 model

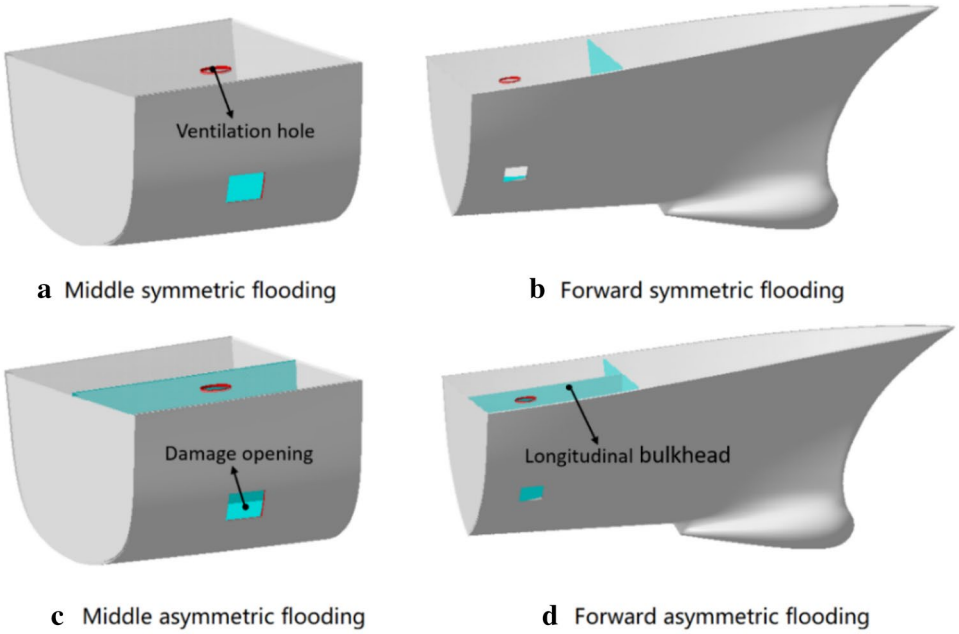

Fig. 7 Different damage scenarios

Table 2 Properties of the hull and specification of the damage opening and ventilation hole

Parameters	Middle symmetric	Middle asymmetric	Forward symmetric	Forward asymmetric
Ventilation hole	Radius	40 mm	Radius	40 mm
Damage opening	100 × 80 mm		80 × 60 mm	
Weight (kg)	709.021	715.576	697.716	705.433
Center of mass x (mm)	2740.764	2742.108	2688.309	2671.158
Center of mass y (mm)	−0.0260	−0.0260	−0.0270	−0.0270
Center of mass z (mm)	289.722	289.531	293.915	294.124
Inertia moment $I_{xx}\left(\mathrm{kg}\cdot\mathrm{m}^2\right)$	64.4640	64.5280	63.3440	63.4610
Inertia moment $I_{yy}\left(\mathrm{kg}\cdot\mathrm{m}^2\right)$	1927.022	1927.436	1973.956	1993.052
Inertia moment $I_{zz}\left(\mathrm{kg}\cdot\mathrm{m}^2\right)$	1944.451	1944.801	1990.800	2009.779
Actual draft (m)	0.282057	0.283717	0.278845	0.281035

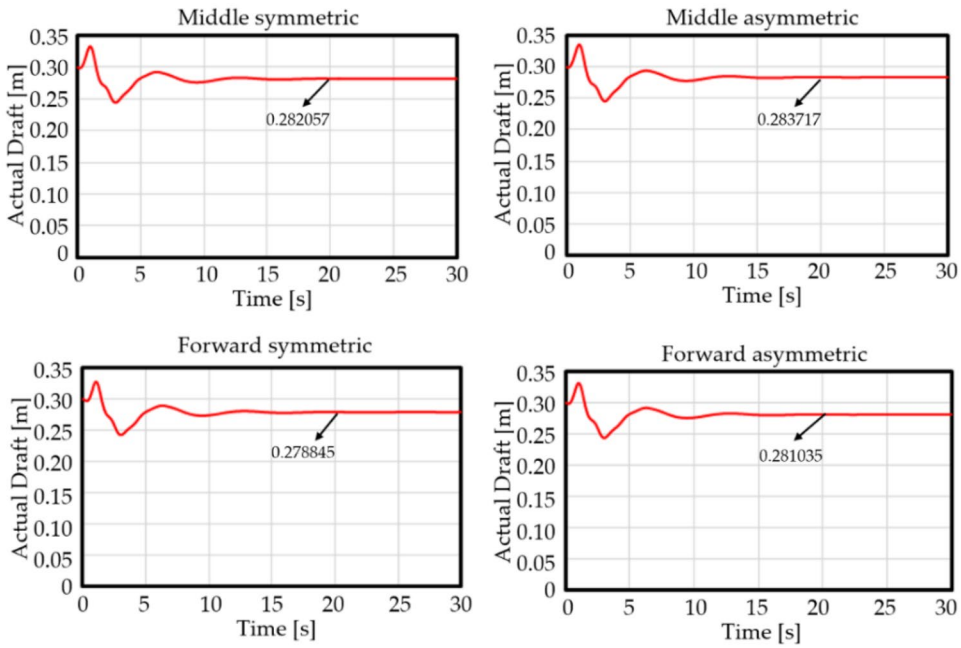

Fig. 8 Actual initial drafts of different damage scenarios

Fig. 8. All the simulation cases are based on the assumption that the ship is placed horizontally. When the damage occurs, the hull may fluctuate up and down due to the transient pitch motion.

6 Numerical setup

In the CFD simulation program, the damaged ship is placed in the limited water area. The limited water area is simulated by a virtual towing tank. As illustrated in Fig. 9, the simulated tank is created by Boolean subtraction operation from the ship and the background region, which is divided into two separate parts by the free surface. Above the free surface is air, and below the free surface is water. When

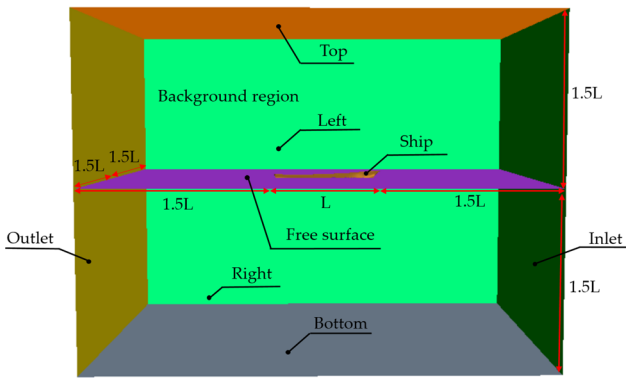

Fig. 9 Domain and boundary representation

this operation is performed, the background region must be defined as the target part. The choice of which body (ship or the background region) to subtract from can lead to two different results. According to the ITTC Recommended Procedures and Guidelines—"Practical Guidelines for Ship CFD Applications" [30], the generated simulation domain is designed as Fig. 9. The detailed dimensions relative to the ship length L are also marked on the schematic diagram. After comprehensive understanding of the published papers [31, 32] and the demonstration case of the KCS Hull with a rudder [23], the appropriate boundary conditions and solver settings are summarized in Table 3. To prevent wave reflection on boundaries, the radiation conditions must be imposed. The simple way to implement no reflection condition is to set the damping wave length on the specific boundaries, including velocity inlet and pressure outlet.

The free surface is modelled with the two phase VOF approach with a High-Resolution Interface Capturing (HRIC) scheme. Through this surface capturing technique, the flooding process coupled with the ship motion can be visualized. It is worth noting that since the ship has a damage opening, the default initial condition is that the damaged compartment is filled with water at the beginning, even if the lower edge of the damage opening is above the free surface. At this time, it is impossible to monitor the flooding process. In this paper, the User Defined Field Function (UDFF) method is developed to distribute the initial free surface, ensuring that the flooded compartment is filled with air at the beginning. This investigation approach is also consistent with the secondary development trend in the current software industry. To model the transient flooding phenomena, an implicit unsteady solver has been applied to find the field of all hydrodynamics unknown quantities, in conjunction with an iterative solver to solve each time step. According to the practical guidelines for ship CFD application [30] and the gathered experience, the simulation cases in this paper applied a constant physical time-step of 0.004 s, involving 10 inner iterations. In addition, Realizable K-Epsilon turbulence model with a good robustness, and a segregated flow solver have been applied for all simulations. For the ship motions, three degrees of freedom motions are released, including roll, pitch and heave motion. Roll and pitch motions are monitored to compare the effects of transverse and longitudinal flooding forms on the damage stability. The heave motion is used to explain the effect of the flooding quantity on the ship sinkage.

In order to guarantee the convergence and reliability of the simulation results, except for appropriate physical models, boundary conditions and simulation solvers, the optimal mesh generation is also a significant consideration. All the simulation cases in this paper apply the hexahedral trimmed mesh with local refinement. This mesh type provides a good compromise between computational time and simulation accuracy. In order to optimize the discretization of each region and avoid large computational costs, the region around the hull is finer than the far field regions. Since the ventilation hole and the damage opening have large surface curvature, the mesh size around these parts must be refined, ensuring that the generated mesh surface is consistent with the imported geometric surface. This refinement operation avoids the effect of the distorted surface on the calculation results. Figure 10 locally presents the shape of the generated ventilation hole and damage opening. It can be found that the fine mesh size restores the original geometric surface. In addition, mesh in the flooding region must also be refined to accurately capture the complex hydrodynamic behavior (splash, bubble and tumble) in the flooding process.

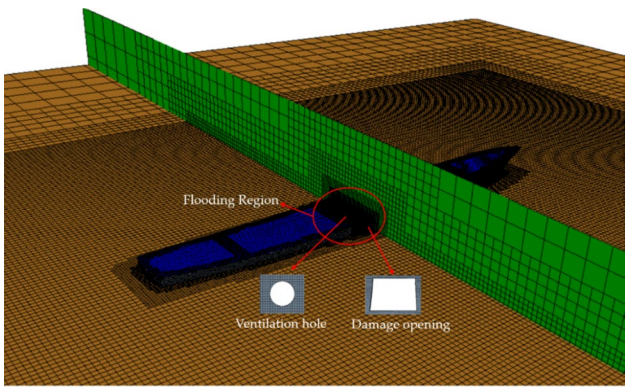

Fig. 10 Mesh visualization around the hull

Table 3 Boundary conditions and solver setting summary

Boundary name	Boundary type (this paper)	Boundary type [31, 32]	Boundary type [23]
Inlet	Velocity inlet	Velocity inlet	Velocity inlet
Outlet	Velocity inlet	Velocity inlet	Pressure outlet
Top/bottom	Velocity inlet	Velocity inlet	Velocity inlet
Left/right	Pressure outlet	Pressure outlet	Symmetry plane
Hull	Wall	Wall	Wall
Convection term	Second-order	Second-order	First-order (default)
Temporal discretization	Second-order	Second-order	First-order (default)

7 Simulation results and discussion

Combined with the simulation settings introduced in the Sect. 6, the damage scenarios described in Sect. 5 are simulated separately. The URANS solver is applied to monitor the 3-DOF coupled motion, including the roll, pitch and heave motion. In this section, the simulation results detail the motion response characteristics of symmetric and asymmetric flooding with different damage locations. The final floating states of the damaged ship in different damage scenarios are visualized by the VOF capturing technique. All the simulation results are based on the assumption that only three degrees of freedom motion is considered. For the side damage flooding scenarios in this paper, the restrained sway motion will have an important influence on the simulation results. The reason for setting such a constraint is that the damaged ship is placed in a limited simulation domain. If the sway motion is released, the damaged ship may move out of the simulation domain, causing the simulation program crash. Therefore, the simulation approach needs further optimization to involve more degrees of freedom motion.

7.1 Analysis of motion responses for the middle damage flooding

Regardless of how a ship is designed, constructed and operated, the ship accidents still keep happening due to a series of reasons. The damage locations are different, including near the bow, the amidship and the stern. In order to comprehensively analyze the flooding process and motion responses of the damaged ship with different damage locations, it is necessary to conduct the targeted research. In this section, the typical middle damage flooding is studied. It can be seen from the Fig. 4 that when the symmetric flooding occurs, the flooding water flows from the damaged side (starboard) to the intact side (portside). Then, the subsequent water ingress results in continuous impact on the intact hull, making the damaged hull perform a reciprocating roll motion on the intact side. This nonlinear roll motion is consistent with the roll motion curve of the symmetric flooding described in Fig. 11. In the transient stage, a certain amount of the flooding water flows into the flooded compartment. In the first second, the flooding water firstly slammed to the deck closed to the damaged side, making the hull heel towards the damaged side. During the flooding time of 1–8 s, with the increase of the flooding water, the flooding water accumulates on the intact side. The roll motion oscillates on the intact side, and the heel value is positive. After 8 s, the flooding water is relatively calm and the influence on the roll

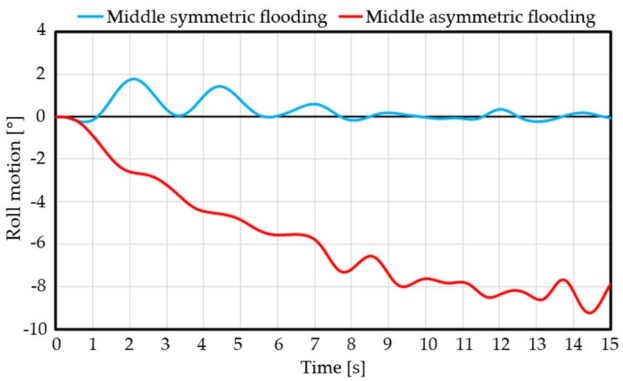

Fig. 11 Roll comparison between middle symmetric and asymmetric flooding

motion can be negligible. The heel value fluctuates slightly above and below 0°. For the middle asymmetric flooding scenario, Fig. 12 presents snapshots of the flooding process at the typical instants. It can be found that during the flooding process, the flooding water continuously have a horizontal impact on the longitudinal bulkhead. This explains why the damaged ship with the asymmetric flooding in Fig. 11 have a slight tendency to heel towards the intact side. However, the flooding water has a greater vertical impact on the bottom deck plate than the horizontal impact on the longitudinal bulkhead. This also explains that the middle asymmetric flooding only cause the damaged ship to heel in the damaged side. Eventually, with the accumulation of the flooding water, the heel angel can reach about 10°. Generally, the middle symmetric flooding and the middle asymmetric flooding only implicate a single damaged compartment. If a more severe damage occurs, two or more damaged compartments may be involved. For the asymmetric flooding, the heel angle can reach 20° or even more. In this case, the excessive heel angle will threaten the safety and survivability of the damaged ship in three aspects. First, the damaged ship is likely to capsize due to the large heel angle. Second, the large heel angle poses a threat to the life safety of the crew on board because the crew cannot maintain a normal walking posture during the evacuation process. Third, some of facilities on board cannot function properly. Especially for the military ships, a large heel angel results in poor missile launching accuracy, which will not guarantee normal combat capability. As shown in Fig. 13, the final heel difference between middle symmetric and asymmetric flooding can be clearly visualized.

For the pitch motion in the middle flooding, the influencing factors are few in the flooding process. As shown in Fig. 14, for the symmetric and asymmetric flooding, the pitch motion curves are essentially consistent during the early flooding stage. Since the default damaged ship is

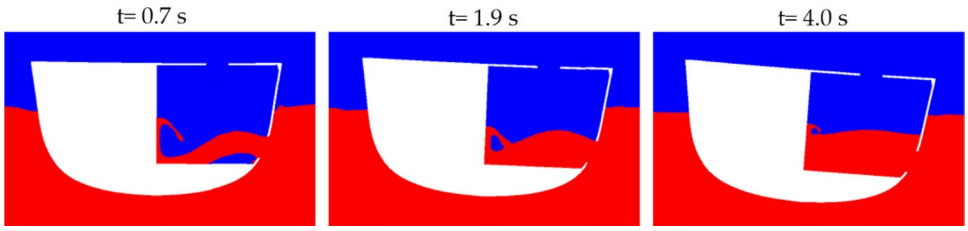

Fig. 12 Snapshots of the middle asymmetric flooding process at the typical instants

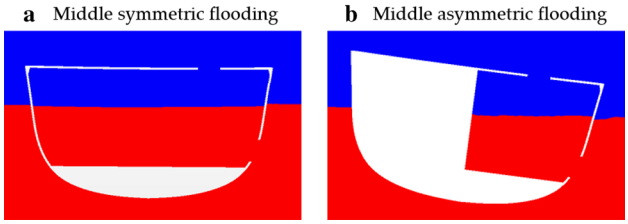

Fig. 13 Final heel difference between middle symmetric and asymmetric flooding

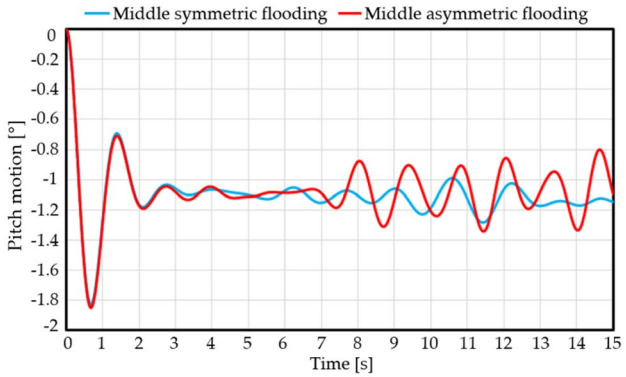

Fig. 14 Pitch comparison between middle symmetric and asymmetric flooding

placed horizontally in the simulation setup, in the first 3 s of the flooding, the pitch motion is mostly caused by the inherent difference between the bow and stern drafts. The damaged compartment is located in the middle of the ship, the additional forces and moment generated by the flooding water are symmetric with respect to the longitudinal direction of the ship. In this case, the hydrodynamics behavior of the flooding water will not have much effect on the pitch motion. However, there are still some differences between the symmetric and asymmetric flooding. This also verifies the pitch motion curve in Fig. 14. As the flooding water increases, the pitch motion under the symmetric flooding is relatively calm. For the asymmetric flooding, the solid–liquid interaction between the flooding water and longitudinal bulkhead results in a greater amplitude of the pitch motion. Similar to the pitch motion, the heave motion of the damaged

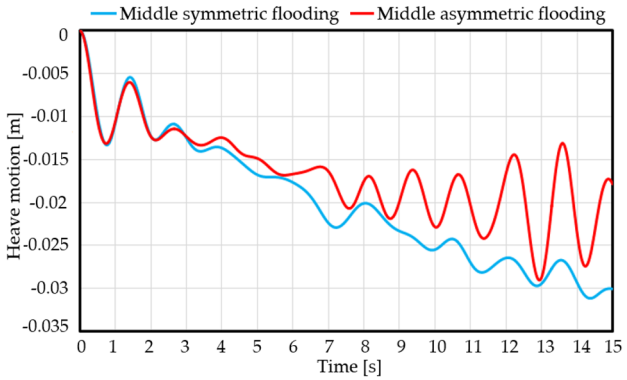

Fig. 15 Heave comparison between middle symmetric and asymmetric flooding

ship is also affected by the inherent difference between the bow and stern drafts. Combined with the right hand rule and the negative value of the pitch angle in Fig. 14, it can be judged that the bow will firstly pitch downward when the damage flooding begins. In addition, the x-direction coordinate of the ship's gravity is about 2.7 m and closer to the bow. In this case, the ship's gravity will sink as the ship pitches towards the bow. Until the maximum sinking limit is reached, the ship will float upward under the action of the buoyancy, and the bow will also pitch upwards. This also explains why the pitch motion and the heave motion curves fluctuate up and down in the first 2 s of the flooding. As shown in Fig. 15, the heave motion curves of the middle symmetric and asymmetric flooding are shown, respectively. It can be found that after experiencing an inherent change of about 2 s, the damaged ship will gradually sink with the increase of the flooding water. Compared to the asymmetric flooding, the symmetric flooding allows more flooding water due to the larger flooded space, causing the damaged ship to sink more. At the same time, corresponding to the pitch curve, the nonlinear hydrodynamics behaviors caused by the asymmetric flooding makes the pitch motion fluctuate more obviously.

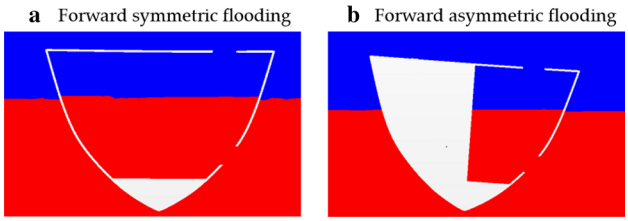

Fig. 16 Final heel difference between forward symmetric and asymmetric flooding

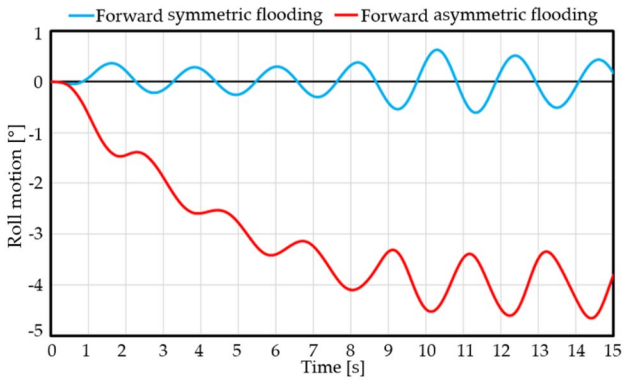

Fig. 17 Roll comparison between forward symmetric and asymmetric flooding

7.2 Analysis of motion responses for the forward damage flooding

In order to comprehensively analyze the effect of damage flooding on the survivability of the ship, another characterized damage scenario, the forward damage flooding, is simulated. Compared with the middle damage flooding, the motion responses under the forward damage flooding both have similarities and differences due to the specified damage location. As shown in Fig. 16, similar to the middle asymmetric flooding, the forward asymmetric flooding also results in a larger heel angel, about 5°. Simultaneously, there is a difference between the middle symmetric flooding and the forward symmetric flooding. Considering Figs. 11 and 17, it can be found that within 1–8 s of the flooding time, the damaged ship under the middle symmetric flooding mostly heels on the intact side. However, for the forward symmetric flooding, the roll motion reciprocates on both sides of the hull. The reason for this difference is related to the geometry shape of the damaged compartment. For the middle symmetric flooding, the damaged compartment is full. The flooding water flows through the internal deck to the intact side and accumulates on the intact side, which explains why the damaged ship in the middle symmetric flooding mostly heels on the intact side within 1–8 s. For the forward symmetric flooding, the cross section of the damages compartment is deep V-shaped. Under the action of the hydrostatic pressure, the flooding water will soon slam the intact side, resulting in the damaged ship to heel towards the portside. At the same time, due to the relatively short transverse distance of the flooded compartment, the flooding water that slams the portside will return to the damaged side. This causes the damaged to heel towards the damaged side again, which explains why the heel value of the forward symmetric flooding in Fig. 17 fluctuates between positive and negative.

Figure 18 partly shows the flooding process of the forward symmetric flooding, which can intuitionally observe the distribution of the flooding water in a certain moment. At 1.5 s, the flooding water slams the portside with a jet form from the damage opening. The flooding water accumulates on the portside, causing the damaged ship to heel towards the intact side. The value of the heel angle is positive. At 2.5 s, the flooding water accumulating on the portside flows to the starboard side, causing the value of the heel angle to be negative. At 4 s, the jet phenomenon turned into the flashy flow, and the continuous flooding water impacts on the intact side with splashing. The damaged ship heels towards the portside, and the value of the heel angle is positive again. In addition, the roll motion curves of the middle asymmetric flooding scenario and the forward asymmetric flooding scenario are of comparative significance. From the Figs. 11 and 17, it can be found that the damaged ship in the forward asymmetric flooding scenario is easier to heel towards the intact side. The amplitude of shaking between the portside and starboard is greater. The reason for this difference is also related to the deep V-shaped damaged compartment. The damage opening is closer to the longitudinal bulkhead. In this case, the horizontal impact of the flooding water on the longitudinal

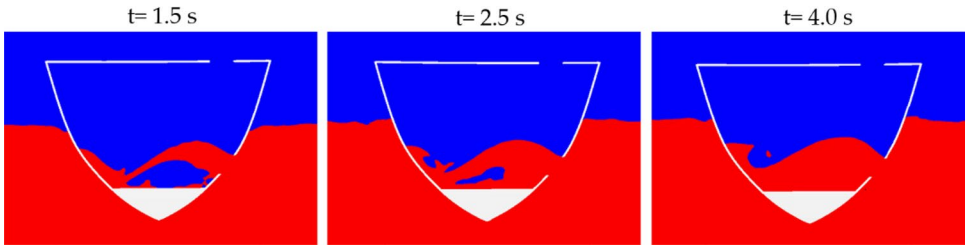

Fig. 18 Snapshots of the forward symmetric flooding process at the typical instants

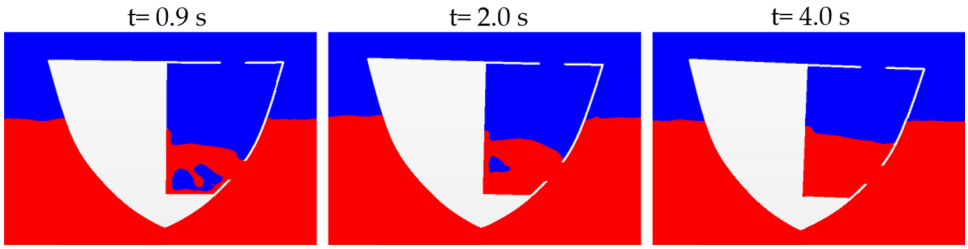

Fig. 19 Snapshots of the forward asymmetric flooding process at the typical instants

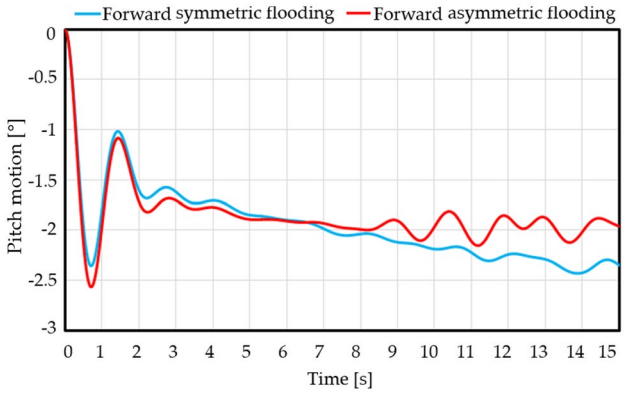

Fig. 20 Pitch comparison between forward symmetric and asymmetric flooding

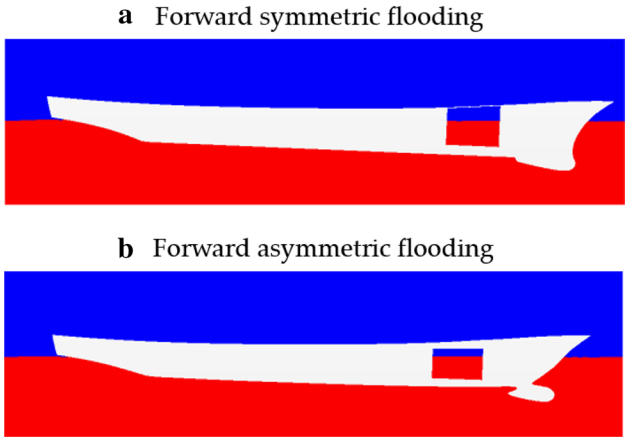

Fig. 21 Final pitch positions of the forward symmetric and asymmetric flooding

bulkhead is greater. The damaged ship is easier to heel towards the portside. Figure 19 presents snapshots of the flooding process at the typical instants. It can be clearly observed that the flooding water impacts the longitudinal bulkhead. Generally, such a visualization process can be an alternative methodology to understand the complex hydrodynamic phenomena in the flooding process, which can also be applied to explain the specified causes of motion behaviors.

Regarding the analysis of the pitch motion under the forward damage flooding, except for the initial pitch angle caused by the inherent difference between the bow and stern drafts, the effect of the asymmetric flooding is also taken into account. As shown in Figs. 14 and 20, the initial pitch angle of the middle symmetric and asymmetric flooding is about 1.8°, while the initial pitch angle of the forward symmetric and asymmetric flooding is about 2.6°. The reasons for this difference include two factors. First, as shown in Table 2, the x-axis coordinates of the gravity in the forward damage scenarios are smaller than the middle damage scenarios. It means that the gravity of the damaged ship in the forward damage scenario is near the bow. In this way, when the forward damage occurs, the initial pitch angle due to the inherent properties of the hull becomes larger than the middle damage scenarios. As shown in Fig. 7, the forward symmetric and asymmetric damage scenarios are generated by modeling the damaged compartment near the bow. The associated bulkheads will locally increase the weight of the bow. Second, when the bow is damaged, the additional force and moment generated by the flooding water are always asymmetric with respect to the longitudinal direction. Such the asymmetric flooding has a worsening effect on the pitch motion. Finally, the pitch angle of the forward symmetric flooding is stable at about 2.5°, and the pitch of the forward asymmetric is stable at about 2°. It can be found that even if the forward symmetric flooding occurs, the final pitch angle is only 2.5°, which will not have much influence on the ship stability. The reason for this phenomenon is that the damaged compartment is not large enough to create a dangerous pitch angle.

Figure 21 presents the final longitudinal floating positions of the forward symmetric and asymmetric damage scenarios. The difference between the two scenarios is small and basically negligible. For the heave motions of the forward symmetric flooding and the forward asymmetric flooding, similar to the middle symmetric flooding, the forward symmetric flooding also accelerates the sinkage of the damaged ship. As shown in Fig. 22, after the initial pitching phase, the forward symmetric flooding allows more flooding water to occupy the damaged compartment, worsening the sinkage of the damaged ship.

Combining the middle damage flooding and the forward damage flooding in this paper, it can be summarized that regardless of the damage location, the transverse

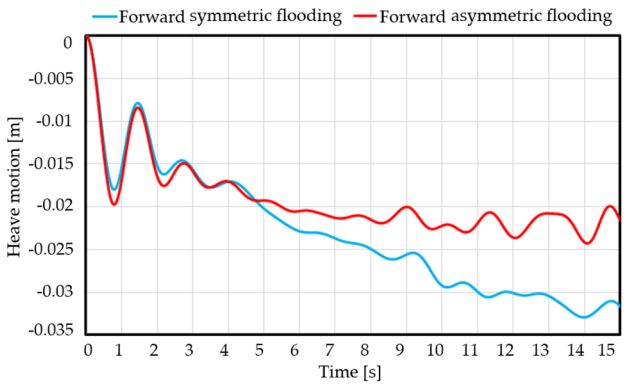

Fig. 22 Heave comparison between forward symmetric and asymmetric flooding

asymmetric flooding makes a larger heel angle, increasing the risk of the damaged ship capsizing. Especially for the middle asymmetric flooding, the heel angle can reach about 10°. Such a heel angle may be a challenge to ensure the normal operation of the damaged ship. However, for the longitudinal asymmetric flooding, except for the inherent initial pitch angel, the same amount of the flooding water has less influence on the pitch motion than the roll motion. If the damaged compartment is not large enough, the pitch difference is basically negligible. Therefore, it can be concluded that when the damage occurs, the transverse asymmetric flooding will be an important consideration for assessing the remaining survivability of the damaged ship. If the damaged ship can maintain a floating state, in order to improve the stability of the damaged ship, the appropriate measures should be taken to allow the flooding water to flow to the other side or to conduct counter measures on the other side. Such measures are already in Safety of Life at sea (SOLAS) regulation on efficient cross-flooding arrangements and allowed time for cross flooding. In this way, the damaged ship can maintain a small heel angle, and the relevant functions onboard can be ensured. This also validate the requirement that in the ship design stage, the cross flooding structures and water diversion equipment should be provided as much as possible. However, if the damaged ship is predicted to be capsized or sinking due to the asymmetric flooding, countermeasures should be taken to block and reduce the flooding. Although the asymmetric flooding can result in a larger heel angle, the flooding time can be extended due to a good flooding limitation. In this case, more flooding time can provide more choices for the rescue management and evacuation option. In general, the numerical simulation method applied in this paper can well capture the flooding process and predict the motion responses of the damaged ship, which provides a good reference for improving the survivability of the ship and optimizing the ship design in the future. However, all the simulation cases are based on the assumption that the damaged compartment is empty, not considering the effect of the permeability on the flooding process and motion responses. In the real compartment layout, there are obstructions and less than 100% permeability in any flooded space. In the future, the real flooding scenarios with complex internal layouts needs to be further studied.

8 Conclusion and future research

The paper demonstrated the feasibility of CFD simulations to investigate complex flooding phenomena. The URANS solver is implemented to solve the 3-DOF coupled motion of the damaged ship. The applied numerical approach can visualize the flooding process, detailing the flooding characteristics of each flooding stage. The various hydrodynamic behaviors in the flooding process are captured, including splashing, bubble and tumble. From the simulation results, it can be summarized that under the same damage condition, the roll motion of the asymmetric flooding may increase the risk of the damaged ship capsizing than the pitch motion. At the same time, the symmetric flooding scenario allows more flooding water to occupy the damaged compartment, worsening the sinkage of the damaged ship. This also validates the existing statement that if the damaged ship is predicted to keep afloat, the cross flooding structure is helpful to improve the survivability of the damaged ship. In this case, the damaged ship can maintain a small heel angle. If the damaged is predicted to capsize and sink, the appropriate counter measures should be taken to prevent the spread of the flooding water as much as possible. Generally, the simulation results can provide a good theoretical basis and investigating method for enhancing the understanding of the damage flooding.

From the perspective of the simulation accuracy, only numerical results have been introduced, without comparison with experimental data. Subsequently, model tests combined with numerical simulation will be performed to validate the reliability of the simulated results. In the future, the flooding process and motion responses under more complex sea conditions will be studied, including wind, beam wave, following or head waves. Damaged stability for the self-propelled free running ship will be investigated. For the mesh processing techniques, more novel methods will be applied, such as overset mesh or DFBI deformation mesh. Additionally, the motion solver needs further optimization to solve more degrees of freedom motion responses, including the sway, surge and yaw motion.

Acknowledgements This research was supported by College of Shipbuilding Engineering, Harbin Engineering University. All the simulation calculations were funded by the National Natural Science Foundation of China (NSFC Grant 51709063).

References

1. Manderbacka T, Themelis N et al (2019) An overview of the current research on stability of ships and ocean vehicles: the STAB 2018 perspective. Ocean Eng 186:106090
2. The specialist committee on prediction of extreme ship motions and capsizing (chaired by D. Vassalos). In: Proceeding of the 27th International Towing Tank Conference (ITTC), Venice, Italy, 2002.
3. Stability in Waves Committee, Final Report and Recommendation (chaired by P.Gualeni). In: Proceeding of the 28th International Towing Tank Conference (ITTC). Wuxi, China, 2017.
4. Cho SK, Sung HG, Hong SY, Nam BW, Kim YS (2010) Study on the motions and flooding process of a damaged ship in waves. In: Proceedings of the 11th International Ship Stability Workshop, Wageningen, Netherlands.
5. Korkut E, Atlar M, Incecik A (2004) An experimental study of motion behavior with an intact and damaged Ro-Ro ship model. Ocean Eng 31:483–512
6. Acanfora M, De Luca F (2017) An experimental investigation on the dynamics response of a damaged ship with a realistic arrangement of the flooded compartment. Appl Ocean Res 69:192–204
7. Domeh VDK, Sobey AJ, Hudson DA (2015) A preliminary experimental investigation into the influence of compartment permeability on damaged ship response in waves. Appl Ocean Res 52:27–36
8. Siddiqui MA, Greco M, Lugni C, Faltinsen OM (2019) Experimental studies of a damaged ship section in forced heave motion. Appl Ocean Res 88:257–274
9. Lee S, You JM, Lee HH, Lim T, Rhee SH, Rhee KP (2012) Preliminary tests of a damaged ship for CFD validation. Int J Nav Archit Ocean Eng 4:172–181
10. Manderbacka T, Vitola M, Celis C, Matusiak JE, Neves MAS, Esperança PTT (2013) Influence of sloshing on the transfer of water between neighbouring compartments considering three different opening configurations. In: Proceeding of 32nd International Conference on Ocean, Offshore and Arctic Engineering. Nantes, France, 9–14 June.
11. Gao Z, Vassalos D, Gao Q (2010) Numerical simulation of water flooding into a damaged vessel's compartment by the volume of fluid method. Ocean Eng 37:1428–1442
12. Haro MPE, Seo J, Sadat-Hosseini H, Seok WC, Rhee SH, Stern F (2017) Numerical simulations for the safe return to port of a damaged passenger ship in head or following seas. Ocean Eng 143:305–318
13. Sadat-Hosseini H, Kim DH, Carrica PM, Rhee SH (2016) URANS simulations for a flooded ship in calm and regular beam waves. Ocean Eng 120:318–330
14. Ming FR, Zhang AM, Cheng H, Sun PN (2018) Numerical simulation of a damaged ship cabin flooding in transversal waves with smooth particle hydrodynamics method. Ocean Eng 165:336–352
15. Zhang XL, Lin Z, Li P, Dong Y, Liu F (2019) Time domain simulation of damage flooding considering air compression characteristic. Water 11(4):796
16. Zhang XL, Lin Z, Mancini S, Li P, Li Z, Liu F (2019) A numerical investigation on the flooding process of multiple compartments based on the volume of fluid method. J Mar Sci Eng 7:211
17. Celis MAC, Wanderley JBV, Neves MAS (2017) Numerical simulation of dam breaking and the influence of sloshing on the transfer of water between compartments. Ocean Eng 146:125–139
18. Santos TA, Soares CG (2009) Numerical assessment of factors affecting the survivability of damaged ro-ro ships in wave. Ocean Eng 26:797–809
19. Manderbacka T, Mikkola T, Ruponen P, Matusiak J (2015) Transient response of a ship to an abrupt flooding accounting for the momentum flux. J Fluid Struct 57:108–126
20. Manderbacka T, Matusiak J, Mikkola T (2015) Study of damping effect of the floodwater on a damaged ship roll motion. In: Proceeding of 25th International Ocean and Polar Engineering Conference 3: 945–951, Kona, Big Island, Hawaii, USA, June
21. Acanfora M, Begovic E, De Luca F (2019) A fast simulation method for damaged ship dynamics. J Mar Sci Eng 7:111
22. Fonfach JM, Manderbacka T, Neves MAS (2016) Numerical sloshing simulations: comparison between lagrangian and lumped mass models applied to two compartments with mass transfer. Ocean Eng 114:168–184
23. STAR-CCM+ Users' Guide version 12.02. CD-Adapco, Computational Dynamics-Analysis & Design Application Company Ltd: Melville, NY, USA.
24. Wood CD (2013) Compartment Flooding and Motions of Damaged Ships. Doctoral Dissertation, University of Southampton.
25. Bulian G, Lindroth D, Ruponen P, Zaraphonitis G (2016) Probabilistic assessment of damaged ship survivability in case of grounding: development and testing of a direct non-zonal approach. Ocean Eng 120:331–338
26. Jalonen R, Ruponen P, Weryk M, Naar H, Vaher S (2017) A study on leakage and collapse of non-watertight ship doors under floodwater pressure. Mari Struct 51:188–201
27. Ruponen P, Kurvinen P, Saisto I, Harras J (2013) Air compression in a flooded tank of a damaged ship. Ocean Eng 57:64–71
28. Cao XY, Ming FR, Zhang AM, Tao L (2018) Multi-phase SPH modelling of air effect on the dynamic flooding of a damaged cabin. Comput Fluids 163:7–19
29. Palazzi L, De Kat J (2004) Model experiments and simulations of a damaged ship with air flow taken into account. Mar Technol 41:38–44
30. Practical Guidelines for ship CFD Application (2011) In: Proceeding of the 26th International Towing Tank Conference (ITTC). Rio de Janerio, Brazil, 28 August-3 September.
31. Begovic E, Day AH, Incecik A, Mancini S (2015) Roll damping assessment of intact and damaged ship by CFD and EFD methods. In: Proceeding of 12th International Conference on the Stability of Ships and Ocean Vehicles, Glasgow, UK, 19–24 June.
32. Mancini S, Begovic E, Day AH, Incecik A (2018) Verification and validation of numerical modelling of DTMB 5415 roll decay. Ocean Eng 162:209–223